Astronomical Observation between Diffraction Limited Coherent and Incoherent Imaging Systems

Raaid N. Hassan 1*

Astronomy and Space, College of Science, University of Baghdad, Baghdad, Iraq.

Abstract

Numerical simulations are carried out to evaluate the coherence concept's effect on the performance regarding the optical system, when observing and imaging the planet's surface. In numerous optical approaches, the coherence qualities of light sources play an important role. This paper provides an overview about the mathematical formulation of temporal and spatial coherence and incoherence properties of light sources. The circular aperture was used to describe the optical system like a telescope. The simulation results show that diffraction-limited for incoherent imaging system certainly improves the image. Yet, the quality of the image is degraded by the light source's highly spatial and temporal coherence properties, resulting in a blurred image with certain parts unresolved, as well as destructive and constructive interference resulting in "ringing" features. When subjective fidelity criteria like PSNR, MSE, SNRrms, SR, R Closeness, and CORR are used to compare the resolution of incoherent and coherent imaging systems, incoherent imaging is often deemed to be "better".

Key Words: PSF, ASF, OTF, Coherent, and Incoherent light.

Number: 10.14704/nq.2022.20.7.NQ33074 **Neuro Quantology 2022; 20(7):574-579**

Introduction

Mesoscopic physics can be defined as the study of quantum electronic phenomena, in the atomic domain, that are realized low dimensional nanostructures ranging from tens of nanometers up to micrometers. The heat flow in these structures had become a very interesting research topic for attractive and viable reasons [1,2]. The heat produced in such dimensions may be broken down the structures' stability. This problem leads many researchers to investigate and understand the heat generation and heat transport in nanodevices coupled to phonon bath [3]. The heat is exchanged with the environment through contact electron reservoirs and phonon bath [4].

Concepts of Coherence

In numerous optical approaches, the coherence qualities of light sources play an important role. The Wiener–Khintchin theorem is utilized in the coherence theory regarding the optical fields to determine the temporal coherence (TC) function [4, 5]. The van-Cittert–Zernike theorem is utilized to determine the lateral spatial coherence (SC) function [6]. The more generalized variant of van-Cittert–Zernike theorem might be used to calculate longitudinal spatial coherence (LSC), which is distinctive from lateral SC [7, 8].

Temporal Coherence

Constant and fixed phase relationship, in other words, the correlation between the light vibrations at two separate points in distinct time, is described

by temporal coherence. Autocorrelation or temporal coherence function, according to the Wiener-Khintchin theorem [5]:

$$\Gamma(\Delta t)=\langle E(t)\, E^{*}(t-\Delta t)\rangle \quad \ldots(1)$$

The power spectral density of the source is formed. The next connection describes the Fourier transform pairings [7- 9]:

$$\Gamma(\Delta t) = \int_{-\infty}^{\infty} S(v) \exp(i2\pi v \Delta t)\, dv \quad \ldots (2)$$

In which, Γ(Δt) represents the temporal coherence function, S(v) represents the source spectral distribution function, and Δt represents the temporal delay between optical fields $E(t)$and $E^*(t-\Delta t)$.

The temporal coherence function's full width half maximum (FWHM) offers information regarding the coherence length. Eq. (2) shows that a higher spectral bandwidth of the light source results in a shorter coherence length or the other way around [10].

Spatial Coherence

Spatial coherence describes the correlation of optical fields at two different spatial locations, situated either transverse or longitudinal direction of the beam propagation, at the same moment of time. It can be seen from the spectral bandwidth of the light source controls the temporal coherence function. In contrast, spatial coherence function is decided by angular frequency spectrum, i.e., number of spatial frequency contained in the light source [11, 12]. In other words, source size controls the spatial coherence function.

Fig. 1 is the manifestation for determining the transverse and longitudinal spatial coherence function of an extended source. Consider the representation of an object as a collection of randomly-radiating point sources.

Incoherent Imaging Theory

Although the item might be illuminated via a source such as the sun, the field exiting object's surface eventually consists of a spectrum of wave-lengths with a randomly shifting phase in time. Because the interference patterns crated via such source type aren't stationary, yet change fast, a sensor responding to field's time-averaged squared magnitude "averages" them out. The term "perfectly incoherent light" indicates a condition in which the complex field phasors from radiating point sources are stochastically independent, without correlation between them at various sites or times. With enough averaging the image texture will tend to become smooth. Assuming incoherent illumination of an object, the linear, space invariant model for imaging becomes [13, 14]:

$$I_i(u,v) = |h(u,v)|^2 \otimes I_g(u,v) \quad \ldots (3)$$

In which, h represents the coherent impulse response function and *Ig* represents the image of the optimal geometric irradiance. Contrary to the coherent imaging that is linear with the field, incoherent imaging is linear with the irradiance. Also, impulse response $|h(u, v)|^2$ has been majorly referred to as point spread function (PSF). The corresponding spectra related to functions in Eq. (3) are related by:

$$G_i(f_u, f_v) = H(f_u, f_v) G_g(f_u, f_v) \quad \ldots (4)$$

where H is known as the optical transfer function (OTF). By convention, the OTF is normalized as follows [15, 16]:

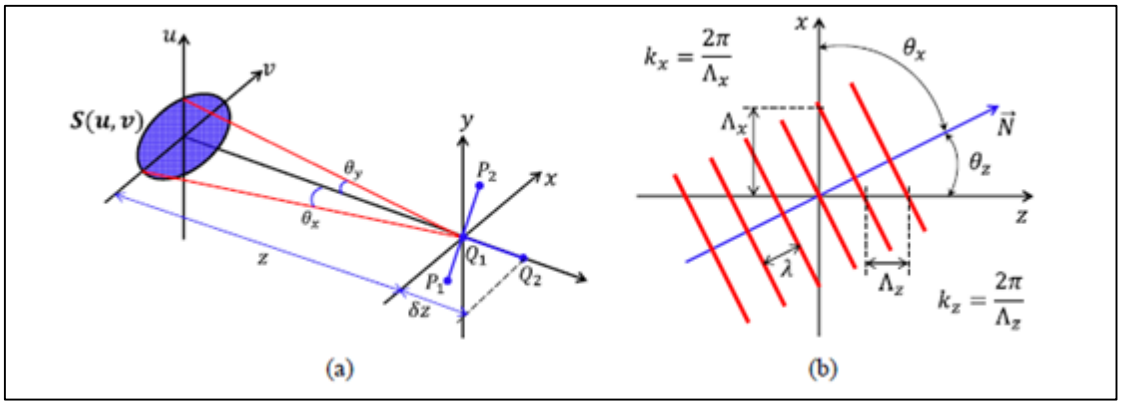

Figure 1. a) Aspect for determining transfers and longitudinal spatial coherence function of extended object. **b)** Spatial periods and spatial frequencies of plane wave propagation [9].

NeuroQuantology | July 2022 | Volume | Issue | Page | doi:
Raaid N. Hassan / Astronomical Observation between Diffraction Limited Coherent and Incoherent Imaging Systems

$$H(f_u, f_v) = \frac{F\{|h(u,v)|^2\}}{\iint_{-\infty}^{+\infty} |h(u,v)|^2 \, dudv} \quad \dots (5)$$

Taking into consideration the Fourier auto-correlation theorem for numerator, OTF is a normalized auto-correlation of the coherent transfer function $H(fu, fv)$. The normalization amounts to scaling the OTF to have a value of 1 at the DC frequency, $(fu, fv) = (0,0)$. This means that the total optical power related to the ideal geometrical image isn't expected to be affected by the OTF.

In shorthand notation, where O indicates the autocorrelation, the OTF can be written as:

$$\mathcal{H}(f_u, f_v) = H(f_u, f_v) O H(f_u, f_v)|_{norm} \quad \dots (6)$$

As image quality measurements, the incoherent PSF and the coherent ASF are explored and presented. Space-variant imaging is caused by aberrated systems, in which the impulse response varies for each image point. A space-variant image simulation is shown as an example.

Diffraction-Limited Coherent Imaging Simulation

One approach for simulating coherent imaging on the computer is based on Eq.(7) [16, 17]:

$$U_i(u,v) = h(u,v) \otimes U_g(u,v) \quad \dots (7)$$

and implemented as:

$$U_i(u,v) = F^{-1}\left\{H(f_u, f_v) F\{U_g(f_u, f_v)\}\right\} \quad \dots (8)$$

The diffraction-limited simulation requires:

$$2f_0 \leq f_N \quad \dots (9)$$

Where f_N is Nyquist frequency and f_0 is coherent cutoff frequency. The coherent transfer function for circular pupil function is given by [18, 19]:

$$H(f_u, f_v) = circ\left(\frac{\sqrt{{f_u}^2 + {f_v}^2}}{f_0}\right) \quad \dots (10)$$

To observe or record a coherent astronomical image, the irradiance given by $I_i = |U_i|^2$ is evaluated. Due to the squaring operation, irradiance astronomical image might theoretically gain up to twice the field's frequency content [20].

Simulation of Diffraction- Limited Incoherent System

The incoherent image simulation according to Eq.(3) could be carried out as [18, 21]:

$$\boldsymbol{I_i(u,v) = F^{-1}\left\{\mathcal{H}(f_u, f_v) F\{I_g(u,v)\}\right\}} \quad \dots (11)$$

The incoherent simulation follows the same form as the coherent case since the OTF is designed from coherent transfer function, while criterion of Eq.(9) can still apply.

The OTF is calculated by applying the autocorrelation theorem for the circular pupil function for the coherent transfer function in Eq. (10)

Numerical Simulation Results

Part1) Diffraction-limited for coherent imaging

1. The ideal image that was taken a 500 × 500 pixel saturn.jpg image. A square image with an even number of samples down each side is excellent. The ideal test image is shown in Fig. 2.

NeuroQuantology | July 2022 | Volume | Issue | Page | doi:
Raaid N. Hassan / Astronomical Observation between Diffraction Limited Coherent and Incoherent Imaging Systems

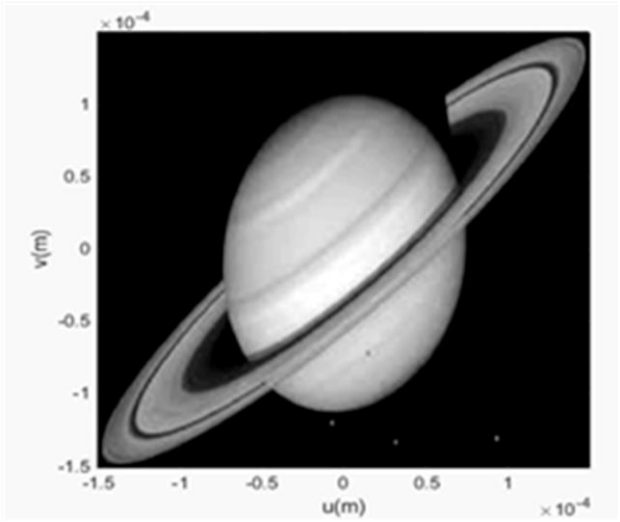

Figure 2. The ideal test image

2. The ideal image represents an irradiance image, took the square root to get the magnitude of the field.
3. Zero phase is assumed across the ideal image.
4. Visible wavelength illumination is assumed with lambda=0.5*10^-6 m.
5. Define the parameters of the imaging system and create the coherent transfer function. The coherent (amplitude) transfer function is displayed in Fig. 3.
6. Eq. (7) is carried out, the subsequent convolution image is shown in Fig. 4 square root of the irradiance is applied to boost the contrast. The features are blurred and some of the arcs are unresolved. Constructive and destructive interference produce "ringing" features.
7. The plot compares simulated and ideal image profiles as shown in Fig. (5).
8. Despite the fact that the irradiance is calculated using the field's square magnitude, the apparent resolution in such type of simulated coherent irradiance image is generally near to coherent cut-off.

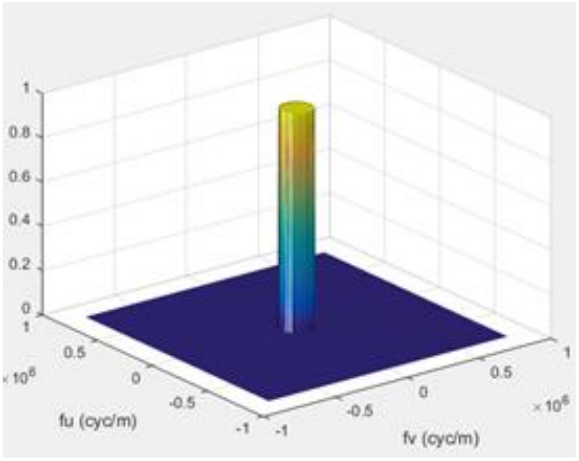

Figure 3. Amplitude transfer function.

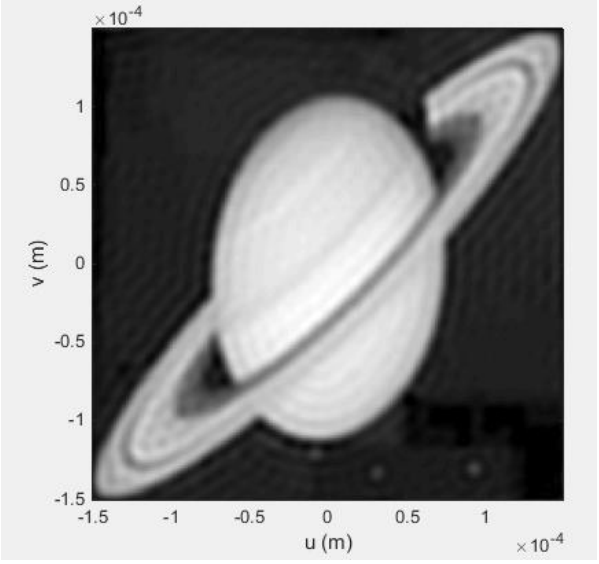

Figure 4. Diffraction-limited coherent image (convolved image).

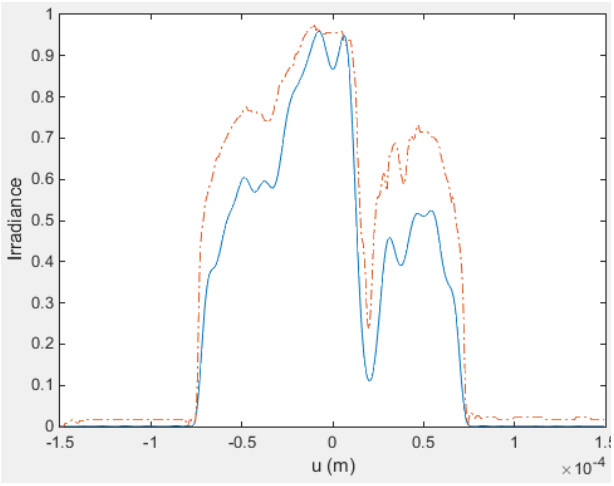

Figure 5. Cross section profile of an ideal image (red dash) and simulated coherent image (blue line).

Part2) Diffraction-limited for incoherent imaging

The incoherent simulation follows the same form as the coherent case since the OTF is created from the coherent transfer function.

1. OTF is calculated by applying the autocorrelation theorem.
2. OTF is normalized by the zero-frequency value of the autocorrelation result.
3. The diffraction-limited OTF is shown in Fig. (6) and the resulting convolved image can be seen in Fig.(7).
4. Compared to coherent image of Fig.(4), the resolution is better and there are no ringing features.
5. The plot compares simulated and ideal image profiles was done in Fig. 8.

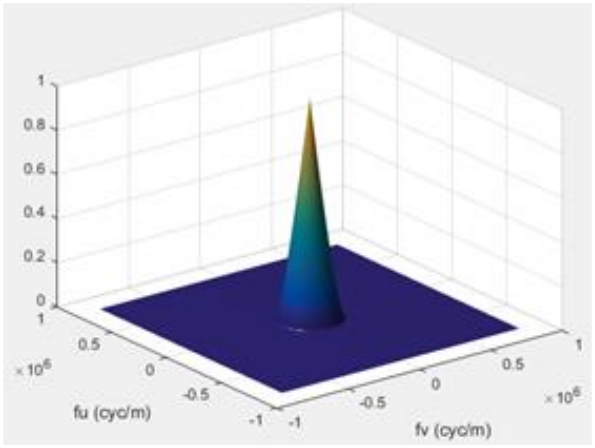

Figure 6. Point Spread Function.

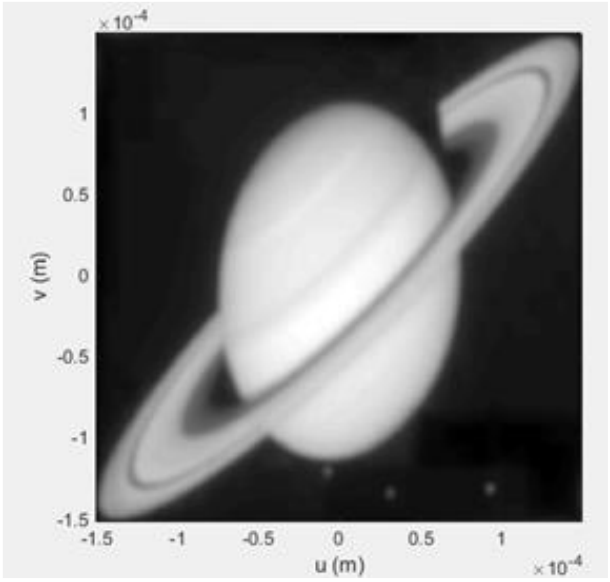

Figure 7. Diffraction-limited incoherent image (Convolved image).

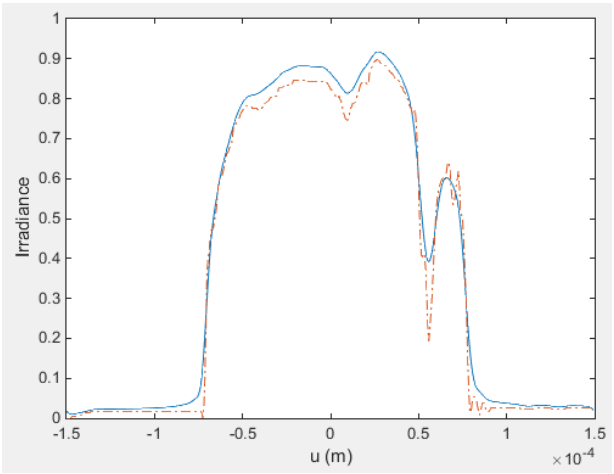

Figure 8. Cross section profile of an ideal image (red dash) and simulated incoherent image (blue line).

Table 1. The fidelity criteria of diffraction-limited coherent and incoherent imaging system.

No.	Fidelity criteria	Coherent image	Incoherent image
1	MSE	0.0192	0.0013
2	SNRrms	2.10	53.38
3	PSNR	17.15	28.81
4	R_Closeness	418.67	476.65
5	SR	0.59	0.948
6	CORR	0.964	0.994

Evaluation with subjective measures necessitates adequate selection of test subjects and well-designed evaluation experimentations for producing unbiased results. Mean square error (MSE), rms of signal to noise ratio (SNRrms), peak signal to noise ratio (PSNR), "R Closeness" is the normalized cross correlation coefficient, estimated Strehl ratio (SR), and correlation coefficients (CORR) are some of the most commonly applied geometric image quality metrics [13]. Table (1) contains some fidelity criteria for comparison between diffraction-limited coherent and incoherent imaging system.

Conclusion

This paper provides an overview about the mathematical formulation of spatial and temporal coherence, and incoherent properties of light sources.

Imaging systems have a linear optical field in the case when the light is coherent. As a result, the image irradiance represents convolution of object irradiance with ASF. The image irradiance is the convolution of the object irradiance with the PSF in the case when light is spatially incoherent. Also, the amplitude spread function's squared magnitude is the point spread function.

Resolution limits criteria are determined by the calculated shape of the PSF associated with the imaging aperture and the wavelength of the light. According to Wiener-Khinchin Theorem, temporal coherence function and source spectrum form pairs of Fourier transform. In other words, larger the bandwidth of source temporal frequency spectrum, smaller will be the coherence length of light source or vice versa.

In this scenario, diffraction-limited incoherent imaging simulation indicates that incoherent light enhances image quality significantly. Yet, the quality of the image is degraded by the light source's strong spatial and temporal coherence qualities, resulting in a blurred image with certain parts unresolved; also, destructive and constructive interference produce "ringing" features, as illustrated in Fig (4). Lastly, subjective fidelity criteria like PSNR, MSE, R Closeness, SNRrms, CORR and SR, are used to compare the resolution of incoherent and coherent imaging systems. Generally, incoherent imaging is considered to be best compared to coherent imaging.

References

1. Edward Steward, Fourier Optics: An Introduction (USA: Dover publications) (2ndEd.) p. 82, (2011).
2. Daniel Wheeler and Jason Schmidt, Applied Optics Vol. 50 p. 3907 (2011).
3. Jason Schmidt, Numerical Simulation of Optical Wave Propagation with Examples in MATLAB (USA: SPIE) p. 39 (2010).
4. Xin Ge, Shufen Chen, Si Chen, and Linbo Liu, Vol. 39 p. 3824 (2021).
5. Valdimir Ryabukho, Dmitrii Lyakin, Yudin Grebenyuk, and Sergey Klykov, Journal of Optics Vol. 15(2) p. 11 (2013).
6. Charles McCutchen, Journal of the Optical Society of America Vol. 56 p. 727 (1966).
7. Anton Grebenyuk, Antoine Federici, Vladimir Ryabukho, and Arnaud Dubois, Applied Optics Vol. 53 p. 1697 (2014).
8. Sultan Wadood, Hugo Schouten, Dylan Fischer, Taco Visser, and Anthony Vamivakas Optics Express Vol. 29 p. 21300 (2021).
9. Sergey Yurish, Advances in Optics: Reviews (Spain: IFSA Publishing) p.491 (2018).
10. Juan Zhao and Wei Wang, Journal of the Optical Society of America A Vol. 31 p. 2217 (2018).
11. Yi Ding and Daomu Zhao Optics Express Vol. 27 p. 32789 (2019).
12. Ari Friberg and Tero Setälä, Journal of the Optical Society of America A Vol. 33 p. 2431 (2016).
13. Hasan. Kondakci, Andre Beckus, Ahmed El Halawany, Nafiseh Mohammadian, George Atia, and Ayman Abouraddy, Optics Express Vol. 25 p. 13087 (2017).
14. David Voels Computational Fourier Optics: a MATLAB tutorial (USA: Published by SPIE) James Harrington p. 7 (2011).
15. Loay Abood, Shatha AL-Hilly, Raaid Hassan, Next generation of Field Aperture Telescope, 2012. Iraqi journal of physics, Vol. 10 (Issue 19), pp.117-132.
16. Tomoyoshi Shimobaba, Takayuki Takahashi, Yota Yamamoto, Takashi Nishitsuji, Atsushi Shiraki, Naoto Hoshikawa, Takashi Kakue, and Tomoyoshi Ito OSA Continuum Vol. 1 p. 642 (2018).
17. Pppria Salami and Leila Yousefi, Journal of Lightwave Technology Vol. 38 p. 2322 (2020).